JOURNAL OF COMPUTATIONAL PHYSICS 107, 40–50 (1993)

Collisional Effects in Plasmas Modelled by a Simplified Fokker–Planck Equation

L. R. T. GARDNER AND G. A. GARDNER

School of Mathematics, University of Wales, UCNW, Bangor, Gwynedd LL57 1UT, United Kingdom

AND

S. I. ZAKI

Department of Mathematics, Suez Canal University, Ismailia, Egypt

Received July 29, 1991

A computer code has been developed to simulate collisional effects in plasmas for the regime where plasma instabilities are dominant but are modified by weak collisions. The numerical method developed for the code is composed of a Galerkin method embedded within a locally one-dimensional approach. This algorithm is used to solve, over the (x, v) phase plane, a simplified Fokker–Planck equation with a one-dimensional Fokker–Planck operator, including a velocity dependent collision frequency. A stability analysis for the numerical scheme is given. The effects of small angle collisions on the Landau damping of plasma waves and the two-stream instability are examined. Results confirm and extend earlier numerical observations.

1. INTRODUCTION

A more complete treatment of the physics of plasmas than that possible with the Vlasov equation requires the solution of the linearised Boltzmann equation with a Fokker–Planck collision term [1] to allow for the electron–electron and electron–ion encounters. The effect of these small angle collisions is of great importance in the physics of fully ionized plasma and should, if possible, be taken into account when simulations of these plasmas are set up [1]. In the present work we have chosen to approximate this requirement by using a simplified one-dimensional Fokker–Planck model as suggested by Lenard and Bernstein [2] and subsequently employed by various other authors [3–11]. This one-dimensional collision operator has the form [10]

$$\left.\frac{\partial f}{\partial t}\right|_c = \frac{\partial}{\partial v}\left(\beta v f + D\frac{\partial}{\partial v}(f\beta)\right), \tag{1}$$

where the collision frequency β may be a function of velocity v, allowing a dependence of the form $\beta \sim 1/v^3$ corresponding to Coulomb collisions, and D is a diffusion coefficient. In (1) the first term accounts for a velocity dependent friction force due to collisions, which tends to slow the particles down and so reduces the kinetic energy. The second term describes the diffusion of particles in velocity space which leads to an increase in kinetic energy. Conservation of energy is obtained by choosing an appropriate form for D. The velocity diffusion is important in the collisional damping of plasma waves and the evolution of the distribution function f of resonant electrons resulting from Landau damping of plasma waves.

This model was used by Lenard and Bernstein [2] in an analysis of collisional damping of plasma waves and by Zakharov and Karpman [8] and also by Denavit, Doyle, and Hirsch [5] in numerical and analytic studies of Landau damping. A collision frequence *independent* of velocity was used in all these studies. Rathmann and Denavit [10] and Mehlhorn and Duderstadt [11] have used velocity dependent collision frequencies in their studies of collisional effects in plasmas. Numerical solutions of the three-dimensional Fokker–Planck equation have been undertaken by Killeen and Marx [9]. This allows more realistic representation of collisions than is possible with the one-dimensional model at the cost of more complex calculations.

For the present work the collision frequency β in Eq. (1) is taken to have the form [10]

$$\beta = \frac{C}{(2\langle v^2\rangle + v^2)^{3/2}}, \tag{2}$$

where C is a collisional constant and

$$\langle v^2\rangle = \frac{1}{n}\int v^2 f\,dx\,dv, \qquad \text{where} \quad n = \int f\,dx\,dv. \tag{3}$$

0021-9991/93 $5.00

From energy conservation considerations it is found that the diffusion coefficient D is now given by [10]

$$D=\frac{\langle\beta v^2\rangle}{\langle\beta\rangle}, \tag{4}$$

where

$$\langle\beta\rangle=\frac{1}{n}\int \beta f\,dx\,dv,$$
$$\langle\beta v^2\rangle=\frac{1}{n}\int \beta v^2 f\,dx\,dv. \tag{5}$$

Although this result was originally derived for a spatially homogeneous plasma [10], an analysis along similar lines shows it to remain true for the present model. When the collision frequency β does not depend upon velocity (4) reduces to $D=\langle v^2\rangle$.

Published numerical solutions of the Fokker–Planck equation are based mainly upon finite difference and transform methods [3–11] but two-dimensional finite elements have been used for the Vlasov equation [12, 13]. More recently we have successfully applied a locally one-dimensional method to the solution of the Vlasov equation [14]. Here a Galerkin formulation incorporating a splitting technique is used to set up a locally one-dimensional finite element solution to the Fokker–Planck equation over the two-dimensional (x, v) phase plane. This approach has been adopted since to obtain accurate solutions to realistic problems the conventional two-dimensional approach makes very heavy demands upon computer storage and CPU time.

2. THE GOVERNING DIFFERENTIAL EQUATIONS

A normalized version of the simplified Fokker–Planck equation for a single species system in one dimension is

$$\frac{\partial f}{\partial t}+v\frac{\partial f}{\partial x}-E\frac{\partial f}{\partial v}=\left.\frac{\partial f}{\partial t}\right|_c, \tag{6}$$

$$\frac{\partial E}{\partial x}=1-\int_{-\infty}^{+\infty} f\,dv, \tag{7}$$

where $f(x, v, t)$ is the distribution function for electrons moving with velocity v in the x direction. The variables have been normalized in the following way: $x\to x/\lambda_D$. $t\to t\omega_p$, $v\to v/v_0=v/(\lambda_D\omega_p)$, $E\to E/(4\pi n_0 e\lambda_D)$, $f\to f/(n_0 e\lambda_D)$; the Debye length $\lambda_D=\sqrt{KT_e/4\pi n_0 e^2}$ and the plasma frequency $\omega_p=\sqrt{4\pi n_0 e^2/m_e}$, where T_e is the electron temperature and n_0, v_0, m_e, e are the electron number density, thermal velocity, mass, and charge, respectively. The ions are assumed to form a fixed neutralizing background. The term

$$\left.\frac{\partial f}{\partial t}\right|_c$$

measures the effect of small angle collisions. The boundary conditions which we have chosen to implement make f periodic in the x direction and allow $f\to 0$ as v becomes large.

The numerical solution method we will describe is based upon the work of Peaceman and Rachford [15] and Marchuk, D'Yakanov, and Yanenko [16] for finite difference methods and is related to the alternating-direction implicit methods described by Hayes [17]. In this approach a splitting technique, is applied to the two "space like" dimensions x and v of Eqs. (1) and (6) so that the single Fokker–Planck equation is replaced by a pair of coupled one-dimensional equations

$$\frac{1}{2}\frac{\partial f}{\partial t}+v\frac{\partial f}{\partial x}=0, \tag{8}$$

$$\frac{1}{2}\frac{\partial f}{\partial t}-E\frac{\partial f}{\partial v}-\frac{\partial}{\partial v}\left(\beta v f+D\frac{\partial}{\partial v}(f\beta)\right)=0. \tag{9}$$

When the numerical solution is set up Eq. (8) is taken as valid over the first half of a time step and in it f is treated as a function of x only, whereas in Eq. (9), valid over the second half of a time step, f is treated as a function of v only.

3. THE FINITE ELEMENT SOLUTION

The decoupled Fokker–Planck–Poisson system (8), (9), and (7) will be solved over a rectangular region of the $x-v$ phase space bounded by the lines $x=0$, L and $v=\pm v_{\max}$.

Two orthogonal families of linear finite elements are set up lying parallel to the coordinate axes and forming a net over the region. Those lying parallel to the x-axis are called the x-family and those parallel to the v-axis the v-family. These elements have a mutual set of nodes sited at the intersections of the families. There are N_x nodes in the x direction and N_v nodes in the v direction. The values of the distribution function at the nodes are alternately determined by solving either Eq. (8) along the x-family or Eq. (9) along the v-family.

The finite element solution of Eq. (8) is constructed using a space-time Galerkin formulation with weight function $N_i(x)$. For each element we obtain

$$\int_0^t\int_0^l N_i(x)\left[\frac{\partial f}{\partial t}+2v\frac{\partial f}{\partial v}\right]dx\,dt, \tag{10}$$

where the $N_i(x)$ are the shape functions for the interpolation of the distribution function in space.

We normalise time using $t=(\Delta t/2)\tau$ and distance using $x=\Delta x\,\xi$, where Δx, Δt are the linear dimensions of a space-time finite element. Then (10) becomes

$$\int_0^1\int_0^1 N_i(\xi)\left[\frac{\partial f}{\partial\tau}+c\frac{\partial f}{\partial\xi}\right]d\xi\,d\tau, \tag{11}$$

where $c=v\,\Delta t/\Delta x$. Within each space-time finite element the distribution function f^e is interpolated by

$$f^e=\sum_{j=1}^{2} N_j(f_j+\tau\,\Delta f_j), \tag{12}$$

where f_j is the nodal value for node $x=x_j$ at the beginning of a time step and Δf_j is the increment gained over that time step. In the present work we will take the shape functions to be piecewise linear functions of ξ so that

$$N_i=(1-\xi,\ \xi). \tag{13}$$

Using Eqs. (12) and (13) in (11) leads to

$$\sum_{j=1}^{2}\left(A_{ij}^e+\frac{c}{2}B_{ij}^e\right)\Delta f_j+c\sum_{j=1}^{2}B_{ij}^e f_j, \tag{14}$$

where

$$A_{ij}^e=\int_0^1 N_iN_j\,d\xi=\frac{1}{6}\begin{pmatrix}2 & 1\\ 1 & 2\end{pmatrix}, \tag{15}$$

and

$$B_{ij}^e=\int_0^1 N_i\frac{\partial N_j}{\partial\xi}\,d\xi=\frac{1}{2}\begin{pmatrix}-1 & 1\\ -1 & 1\end{pmatrix}, \tag{16}$$

Assembling contributions from all elements along a typical member of the x-family gives

$$\sum_j\left(A_{ij}+\frac{c}{2}B_{ij}\right)f_j^{n+1/2}=\sum_j\left(A_{ij}-\frac{c}{2}B_{ij}\right)f_j^n, \tag{17}$$

which is a set of simultaneous linear equations of tri-diagonal form for updating the nodal values of f_j over the first half of a timestep. The assembled matrices A_{ij} and B_{ij} are the same for each member of the x-family. The variation from member to member being provided only by the parameter $c=v\,\Delta t/\Delta x$.

A typical equation from (17) is

$$\begin{aligned}\left(1-\frac{3c}{2}\right)f_{j-1}^{n+1/2}+4f_j^{n+1/2}+\left(1+\frac{3c}{2}\right)f_{j+1}^{n+1/2}\\ =\left(1+\frac{3c}{2}\right)f_{j-1}^{n}+4f_j^{n}+\left(1-\frac{3c}{2}\right)f_{j+1}^{n},\\ j=1,\ \ldots,\ N_x,\end{aligned} \tag{18}$$

where, for simplicity, all elements in the x-family are chosen to have the same linear dimension Δx.

The finite element [13] solution of Eq. (9) is constructed using a space-time Galerkin formulation with weight function $N_i(v)$. We obtain

$$\int_0^t\int_{-v_{\max}}^{v_{\max}} N_i(v)\left[\frac{1}{2}\frac{\partial f}{\partial t}-E\frac{\partial f}{\partial v}-\frac{\partial}{\partial v}\left(\beta vf+D\frac{\partial}{\partial v}(f\beta)\right)\right]dv\,dt=0.$$

For boundary conditions on f we assume that at $v=\pm v_{\max}$ we have $f=\partial f/\partial v=0$. On integrating by parts and using these boundary conditions we obtain

$$\int_0^t\int_{-v_{\max}}^{v_{\max}} N_i(v)\left[\frac{1}{2}\frac{\partial f}{\partial t}-E\frac{\partial f}{\partial v}\right]+\frac{\partial N_i}{\partial v}\left[\beta vf+D\frac{\partial}{\partial v}(f\beta)\right]dv\,dt=0. \tag{19}$$

Using (4) for β gives

$$\begin{aligned}\frac{\partial}{\partial v}(f\beta)&=\beta\frac{\partial f}{\partial v}+f\frac{\partial\beta}{\partial v}\\ &=\beta\frac{\partial f}{\partial v}-f\frac{3v\beta}{(2\langle v^2\rangle+v^2)}.\end{aligned} \tag{20}$$

We apply the foregoing analysis and obtain the contribution to (19) of a typical element, in terms of local coordinates ξ, τ, where $t=(\Delta t/2)\tau$ and $v=\Delta v(j+\xi)$, in the form

$$\int_0^1\int_0^1\left\{N_i(\xi)\left[\frac{\partial f}{\partial\tau}-c\frac{\partial f}{\partial\xi}\right]+\Delta t\frac{\partial N_i}{\partial\xi}\left(\beta ef(j+\xi)+\frac{D\beta}{\Delta v^2}\frac{\partial f}{\partial\xi}\right)\right\}d\xi\,d\tau, \tag{21}$$

where now $c=E\,\Delta t/\Delta v$ for the typical element $[j\,\Delta v,\ (j+1)\,\Delta v]$ and $e=1-3D/(2\langle v^2\rangle+v^2)$.

Now proceeding as before we obtain a second matrix equation similar in form to Eq. (17) but relating the distribution function at time level $n+1$ to that at time level $n+\frac{1}{2}$. Assembling contributions from all elements along a typical member of the v-family leads to

$$\sum_j\left[A_{ij}-\frac{c}{2}B_{ij}+\frac{be}{2}(jB_{ji}+P_{ij})+\frac{bD}{2\Delta v^2}Q_{ij}\right]f_j^{n+1}=\sum_j\left[A_{ij}+\frac{c}{2}B_{ij}-\frac{be}{2}(jB_{ji}+P_{ij})-\frac{bD}{2\Delta v^2}Q_{ij}\right]f_j^{n+1/2}. \tag{22}$$

Strictly, this is a formal result as both $b=\beta\,\Delta t$ and e are element dependent.

The matrices A_{ij}, B_{ij}, P_{ij}, Q_{ij} are derived from the element matrices (15) and (16), together with

$$P^e_{ij}=\int_0^1 \xi\frac{\partial N_i}{\partial\xi}N_j\,d\xi=\frac{1}{6}\begin{pmatrix}-1 & -2\\ 1 & 2\end{pmatrix},$$

and

$$Q^e_{ij}=\int_0^1 \frac{\partial N_i}{\partial\xi}\frac{\partial N_j}{\partial\xi}\,d\xi=\begin{pmatrix}1 & -1\\ -1 & 1\end{pmatrix}.$$

Once more the variation in the matrix equation from member to member of the v-family is provided by the parameter c which depends only upon the electric field E which is a function only of x and so is constant along each member of the v-family.

A typical member of Eq. (22) is

$$\begin{aligned}&\left(1+\frac{3c}{2}+b_{j-1/2}\left[\left(\frac{3}{2}j-1\right)e_{j-1/2}-3d\right]\right)f^{n+1}_{j-1}\\&\quad+\left(4+b_{j-1/2}\left[\left(\frac{3}{2}j-\frac{1}{2}\right)e_{j-1/2}+3d\right]\right.\\&\quad\left.-b_{j+1/2}\left[\left(\frac{3}{2}j+\frac{1}{2}\right)e_{j+1/2}-3d\right]\right)f^{n+1}_{j}\\&\quad+\left(1-\frac{3c}{2}-b_{j+1/2}\left[\left(\frac{3}{2}j+1\right)e_{j+1/2}+3d\right]\right)f^{n+1}_{j+1}\\&=\left(1-\frac{3c}{2}-b_{j-1/2}\left[\left(\frac{3}{2}j-1\right)e_{j-1/2}-3d\right]\right)f^{n+1/2}_{j-1}\\&\quad+\left(4-b_{j-1/2}\left[\left(\frac{3}{2}j-\frac{1}{2}\right)e_{j-1/2}+3d\right]\right.\\&\quad\left.+b_{j+1/2}\left[\left(\frac{3}{2}j+\frac{1}{2}\right)e_{j+1/2}-3d\right]\right)f^{n+1/2}_{j}\\&\quad+\left(1+\frac{3c}{2}+b_{j+1/2}\left[\left(\frac{3}{2}j+1\right)e_{j+1/2}+3d\right]\right)f^{n+1/2}_{j+1},\\&\qquad j=1,2,\ldots,N_v,\end{aligned}\tag{23}$$

where

$$c=\frac{E\,\Delta t}{\Delta v},\qquad d=\frac{D}{\Delta v^2},$$

$$b_j=\beta\,\Delta t=\frac{C\,\Delta t}{(2\langle v^2\rangle+v_j^2)^{3/2}},$$

$$e_j=1-\frac{3D}{(2\langle v^2\rangle+v_j^2)},$$

$$b_{j-1/2}=\frac{1}{2}(b_{j-1}+b_j),$$

with a similar result for $e_{j-1/2}$. The subscript j denotes the values at node $v=v_j$. All elements in the v direction have the same constant linear dimension Δv.

The original two-dimensional problem would lead to a single matrix equation of size $(N_vN_x\times N_vN_x)$ and bandwidth $(2N_x+3)$. The locally one-dimensional approach replaces this large system of equations by a series of N_v matrix equations of size $(N_x\times N_x)$ and N_x matrix equations of size $(N_v\times N_v)$ all of tridiagonal form, or near tridiagonal form, which are solvable directly by the Thomas algorithm or a variant of it.

In setting up a numerical solution for Poisson's equation it is convenient to write Eq. (7) in the form

$$\frac{\partial E}{\partial x}=\rho,\qquad\text{where}\quad\rho=1-\int_{-\infty}^{\infty}f\,dv.\tag{24}$$

Applying Galerkin's method then leads to the system of equations

$$-E_{j-1}+E_j=\frac{\Delta x}{2}(\rho_{j-1}+\rho_j),\tag{25}$$

where

$$\rho_j=1-\sum_i^{N_v}f(x_j,v_i)\,\Delta v_i$$

and (x_j, v_i) are the coordinates of the nodes. As boundary conditions on the electrostatic field we take the average value of the field to be zero. This leads to a recurrence relationship for the nodal values of the field

$$E_N=E(x_N)=\frac{\Delta x}{2N_x}\sum_{j=1}^{N_x}\rho_j(2j-1),\tag{26}$$

and

$$E_{k-1}=E_k-\frac{\Delta x}{2}(\rho_{k-1}+\rho_k),\qquad\text{where}\quad k=N,N-1,\ldots,2.\tag{27}$$

The solution procedure we have adopted is as follows:

(a) Solve Eq. (18) separately along each line of nodes in the x-family ($v=v_i$) and so update the values of the distribution function to time level $(n+\frac{1}{2})$; that is, determine $f_j^{n+1/2}$.

(b) Use the recurrence relationship (27) to obtain the nodal values of the electric field E, which is a function of x only, for use in the next step.

(c) Solve Eq. (23) separately along each line of nodes in the v family ($x=x_i$, a constant, where $E=E_i$) and so update the values of the distribution function to time level $n+1$, that is determine f_j^{n+1}.

Note that in solving (23) the redistribution of f takes place only in the v direction and so it does not change the values of ρ_j (Eq. (26)); hence the solution of (27) is unaffected and the electric field E remains constant over the second half of the timestep. There is thus no additional approximation introduced in assuming E is constant when using Eq. (23) to update values of f.

No bias has been observed when using this algorithm in the simulations reported here. However, if bias is suspected the updating can be alternated between the x and v directions over two timesteps in the following way:

(a) spatial advance $f^n \to f^{n+1/2}$ using (18),

(b) determine the electric field E from (27),

(c) velocity advance $f^{n+1/2} \to f^{n+1}$ using (23); E is unaffected,

(d) velocity advance $f^{n+1} \to f^{n+3/2}$ using (23); E is unaffected,

(e) spatial advance $f^{n+3/2} \to f^{n+2}$ using (18).

Now repeat above stages (a)–(e) throughout the simulation.

4. PROPERTIES OF THE NUMERICAL SCHEME

We now examine the properties of the numerical scheme (18) and (23).

4.1. *Numerical Stability*

The stability analysis we set up is based on the Neumann theory. We study the effects of the numerical scheme on a Fourier mode of the distribution function

$$f_j^n = \hat{f}^n e^{ijk\Delta},$$

where k is the mode number and Δ takes either the value Δx or Δv. The mode amplitude $\hat{f}$ at successive time levels is related by the equation

$$\hat{f}^{n+1/2} = g\hat{f}^n,$$

where g is the growth factor.

For scheme (18) valid over the first half of a time step g is given by

$$g = \frac{p - iq}{p + iq},$$

where $p = 2\cos k\Delta + 4$ and $q = 3c \sin k\Delta$. Thus $|g| = 1$ and the scheme is unconditionally stable.

If we assume that all the b_j and e_j are locally constant with values b and e, a similar analysis of Eq. (23) leads to a growth factor

$$g = \frac{2(1 + be + 3bd)\cos k\Delta + 4 + be - 6bd + i\alpha}{2(1 - be - 3bd)\cos k\Delta + 4 - be + 6bd - i\alpha},$$

where $\alpha = (3c + 3bej)\sin k\Delta$.

For $\beta = 0$ we find that the scheme is unconditionally stable. When collisions occur, $\beta \neq 0$, and we find the condition for stability is $8be(2 - \cos k\Delta)(2\cos k\Delta - 1) + 48bd(1 - \cos k\Delta)(2 + \cos k\Delta) \geqslant 0$. All the brackets are greater than or equal to zero, except $(2\cos k\Delta - 1)$ which is negative when $\cos k\Delta$ lies in the range $-1 \leqslant \cos k\Delta < \frac{1}{2}$. Thus term two is always positive, while term one becomes negative when $\cos k\Delta < \frac{1}{2}$. When term two is small, through $\cos k\Delta$ being near one, term one is positive. As $\cos k\Delta$ decreases down from one, term two increases in size, whereas term one decreases, by the time $\cos k\Delta < 0$, and term one becomes negative, term two is large enough (as $d/e > 1$) to ensure that the whole expression remains positive. The scheme is therefore unconditionally stable.

4.2. *Conservation*

The first, free streaming, part of the numerical scheme, Eq. (18), conserves particle numbers and the moments of the distribution function.

The second part, Eq. (23), also conserves particle numbers. We now consider moments. Taking the first and second moments of the distribution function along a v-family member produces

$$2\sum_j f_j^{n+1} v_j + \sum_j f_j^{n+1} v_j \beta\, \Delta t + \Delta t\, E \sum_j f_j^{n+1}$$

$$= 2\sum_j f_j^{n+1/2} v_j - \sum_j f_j^{n+1/2} v_j \beta\, \Delta t$$

$$- \Delta t\, E \sum_j f_j^{n+1/2},$$

and, dropping second order terms,

$$\sum_j f_j^{n+1} v_j^2 + \Delta t\, E \sum_j f_j^{n+1} v_j$$

$$- \sum_j f_j^{n+1} D\beta\, \Delta t + \sum_j f_j^{n+1} v_j^2 \beta\, \Delta t$$

$$= \sum_j f_j^{n+1/2} v_j^2 - \Delta t\, E \sum_j f_j^{n+1/2} v_j$$

$$+ \sum_j f_j^{n+1/2} D\beta\, \Delta t - \sum_j f_j^{n+1/2} v_j^2 \beta\, \Delta t.$$

These equations are discrete analogues of

$$\frac{\partial\langle v\rangle}{\partial t}+\langle v\beta\rangle=-\frac{eE}{m}, \tag{28}$$

$$\frac{1}{2}\frac{\partial\langle v^2\rangle}{\partial t}+\frac{eE}{m}\langle v\rangle=D\langle\beta\rangle-\langle v^2\beta\rangle. \tag{29}$$

Equations (28) and (29) are Eqs. (A8) and (A9) from Appendix A of Ref. [10] for a spatially homogeneous one-dimensional plasma. In (29) the left-hand members represent the rate of change of the sum of the one-dimensional kinetic and potential energies and the diffusion coefficient D is chosen to ensure that this sum is conserved. Summing contributions of all v-family members generalises these results to a spatially inhomogeneous one-dimensional plasma.

In the simulations discussed in Section 5 the average value of the self-consistent electric field E is zero and the distribution function is an even function so that $\langle v\rangle=0$ and $\langle v\beta\rangle=0$. It follows from Eq. (28) that the drift velocity $\langle v\rangle$ remains zero and from Eq. (29) that $\langle v^2\rangle$ is conserved.

5. THE SIMULATIONS

We examine the effect of collisions on the physics of one-dimensional plasmas subject to self-consistent electric fields. There are earlier computer simulations which include both self-consistent electric fields as well as collisional effects [18], but that model was based on the Krook collision term in which the distribution function relaxes to a Maxwellian function at a rate which is independent of its gradient in velocity space. The present collision operator includes derivatives which take account of diffusion in velocity which is important when studying the evolution of the distribution function resulting from Landau damping of plasma waves. Two classical problems, Landau damping and the two stream instability, are considered in this study.

For the Vlasov equation ($\beta=0$) the equilibrium distribution function is

$$f_0(v)=(1/\sqrt{2}\,\pi)\exp(-v^2/2). \tag{30}$$

Using this Maxwellian distribution function, with a velocity dependent collision frequency (4), we find that $\langle v^2\rangle$ and D have the approximate values $\langle v^2\rangle=1.5$ and $D=0.68$. When the collision frequency β is independent of velocity $D=\langle v^2\rangle=1$.

It has been shown [10] that for the simplified Fokker–Planck equation discussed here the equilibrium distribution function is given not by (30), but by

$$f_0^E(v,\,t\to\infty)=\left(\frac{1}{\langle v^2\rangle}\right)(2\langle v^2\rangle+v^2)^{3/2}\times\exp(-0.88v^2/\langle v^2\rangle). \tag{31}$$

with an appropriate normalization. For this distribution function we obtain the approximate values $\langle v^2\rangle=1.004$ and $D=0.5692$ leading to $\alpha=\langle v^2\rangle/D=1.754$, which compares very well with the theoretical value of $\alpha=\langle v^2\rangle/D=1.76$ [10]. For this case, since $\langle v^2\rangle$ is constant, Rathmann and Denavit [10] find it convenient to write the collision constant $C=(3\langle v^2\rangle)^{3/2}\nu_0$, where ν_0 may be interpreted as the collision frequency of a particle at the thermal velocity. With other distribution functions, for example (33), these authors use a similar expression [10] for C so that the collision frequency β is always of the form

$$\beta=\frac{(3\langle v_0^2\rangle)^{3/2}\nu_0}{(2\langle v^2\rangle+v^2)^{3/2}}, \tag{32}$$

where $\langle v_0^2\rangle$ is the value at $t=0$, and $\langle v^2\rangle$ is the current value; we shall follow the same practice.

Our first simulation will be of linear Landau damping and we shall use as initial condition [7]

$$f_0(x,\,v,\,0)=f_0(v)(1+A\cos kx), \tag{33}$$

where A is the amplitude of the initial sinusoidal perturbation of wave number k imposed upon the Maxwellian distribution function $f_0(v)$, Eq. (30).

To place the present algorithm in the context of earlier work we first examine a standard problem [7, 14] concerning the relaxation of a small perturbation in the distribution function for the collisionless case, $\nu_0=0$. We use as initial condition (33) and (30) with $A=0.05$, $k=0.5$ so that the plasma has length $L=12.56637$ and we also take $v_{\max}=6$, 32 elements in x and 48 elements in v so that $\Delta v=0.25$. The behaviour of the amplitude of the first mode of the electrostatic field is shown in Fig. 1. It initially decays with a damping rate $\gamma=-0.1537$ and an oscillation frequency $\omega=1.417\,\omega_p$ which compare well with values of $\gamma=-0.1532$ and $\omega=1.4159\,\omega_p$ obtained numerically by Cheng and Knorr [7] and agree well with $\gamma=-0.1533$ and $\omega=1.4156\,\omega_p$ obtained from Landau's dispersion relationship [19]. An approximate recurrence of the initial state occurs at about $t=48(1/\omega_p)$. This effect is well known [7], having been observed in several independent simulations of Landau damping, and has been shown to be due to the finite velocity resolution of the methods. Theory predicts that the recurrence occurs at time $T_R=2\pi/(k\,\Delta v)=48.85(1/\omega_p)$ for the present case.

We have monitored the distribution function and its first two moments throughout the run which lasts until a time $t=75(1/\omega_p)$ and observe good conservation. We find that n

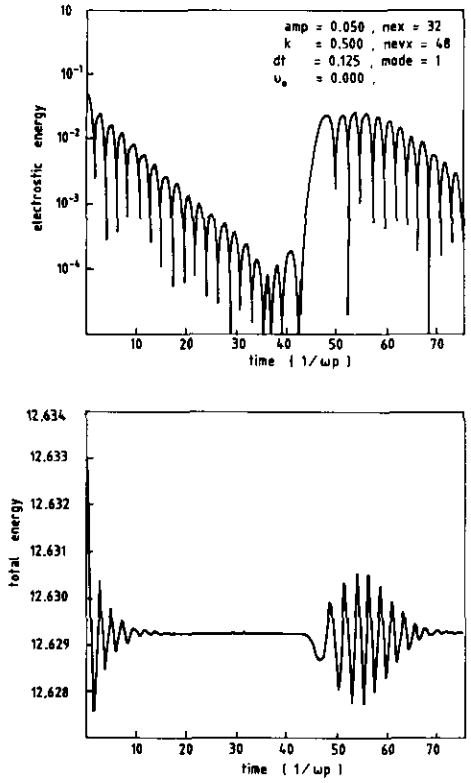

FIG. 1. Collisionless linear damping of a small perturbation. Upper graph shows the variation in the amplitude of $|E_1|$, $k=0.5$, $A=0.05$, $N_x=32$, $N_v=48$, $L=12.56637$, $v_{\max}=6.0$, $dt=0.125$. Lower graph gives variation in total energy.

(Eq. (3)) varies by less than $10^{-4}\%$, $\langle v\rangle$ differs from zero by less than 2×10^{-7}, while $\langle v^2\rangle$ varies by less than 0.08%, and in the period of linear damping $10<t<40$ by less than $3\times10^{-4}\%$. The conservation of energy is also good as can be seen from the graph of the variation in the total energy shown in Fig. 1. There is an initial transient up to 12.633 followed by oscillations of rapidly decreasing amplitude until a constant value of 12.6292 is obtained at about $t=20(1/\omega_p)$. Oscillations reappear in the energy at about T_R but rapidly die away. In all subsequent numerical experiments the velocity step Δv is chosen small enough to ensure that T_R is longer than the run time so that no recurrence effects occur within the simulation period.

This problem has also been solved using the alternate algorithm given at the end of Section 3 and identical results obtained.

To obtain linear damping conditions comparable with those of other authors [5] we have chosen the parameters in (33) to have the values $A=0.05$ and $k=0.3535$. For this choice the length of the plasma is $L=2\pi/k=17.7743$. There are 32 elements in the x direction and 45 in the v direction, $v_{\max}=4.0$. We have examined the effect of a velocity *independent* collision frequency [20], for which $\beta=v_0$, on the time variation of the amplitude of the first electrostatic

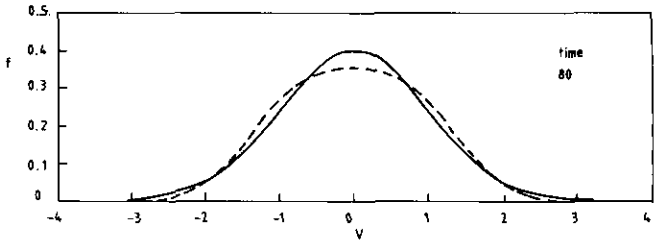

FIG. 2. Linear Landau damping. Distribution function at $t=80(1/\omega_p)$; (———) $v_0=0$, (---) $v_0=0.2$.

mode for collision parameters values of $v_0=0$ and 0.005. Previous investigators [5] determined the time variation of the first mode of the number density. These two set of results are comparable since on Fourier analysing Eq. (2) the amplitude of the number density F_r and electric field E_r modes are related by $E_r=(1/rk)F_r$, where r is the mode number. For the mode considered above $E_1=3F_1$ and the behaviour of the number density mode, see Fig. 6 of Ref. [5], is exactly mirrored in the electrostatic mode in the present simulation. Initially, up to a time of about $30(1/\omega_p)$ both modes decay at nearly the expected linear damping rate of $\gamma=-0.0343$ [19]; thereafter, although the curve for $v_0=0.005$ still shows almost linear decay, the graph for $v_0=0.0$ shows growth. For all values of v_0 the initial modal amplitudes are $F_1=2\times10^{-2}$ and $E_1=6\times10^{-2}$. At a later time of about $60(1/\omega p)$ we find that for $v_0=0.0$, $F_1=1\times10^{-2}$ and $E_1=3\times10^{-2}$, while for $v_0=0.005$, $F_1=1.4\times10^{-3}$ and $E_1=4\times10^{-3}$. These values satisfy the relationship discussed above. There is agreement between our results and those of Denavit *et al.* [5]; see their Fig. 6. The Maxwellian distribution function remains smooth and symmetric about $v=0$. The graph of total energy shows this to be conserved to better than 0.1% in each simulation.

When a velocity *dependent* collision frequency of the form (32) is used in a similar simulation the symmetric distribu-

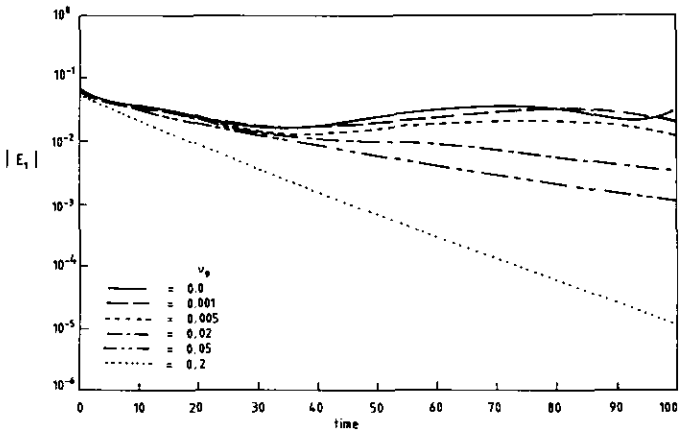

FIG. 3. Linear Landau damping. Electrostatic mode $|E_1|$, $k=0.3535$, $A=0.05$, $N_x=32$, $N_v=45$, $L=17.7743$, $v_{\max}=4.0$, $dt=0.125$. The collision frequency v_0 has the values $v_0=0$, 0.001, 0.005, 0.02, 0.05, 0.2.

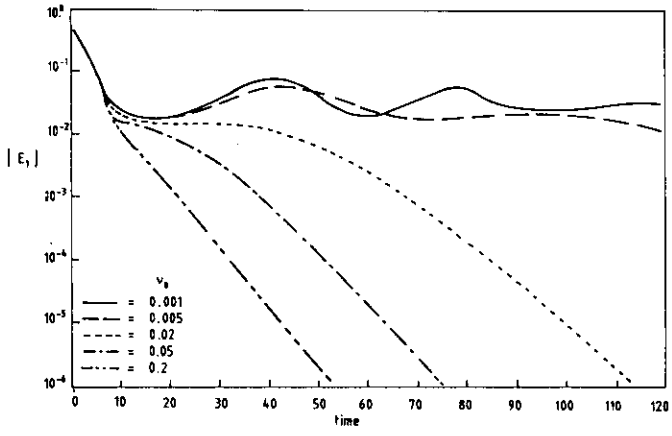

FIG. 4. Non-linear Landau damping. Electrostatic mode $|E_1|$, $k = 0.5$, $A = 0.5$, $N_x = 32$, $N_v = 128$, $L = 12.5664$, $v_{max} = 5.0$, and $dt = 0.125$. Collision frequencies $v_0 = 0.001, 0.005, 0.02, 0.05, 0.2$.

tion function broadens and flattens as seen in [10]; see Fig. 2. The amount of broadening varies with the size of the collision frequency. In Fig. 3 the *envelope* of the amplitude of the first mode of the electric field is shown. For the collisionless model we observe an initial damping with rate $\gamma = -0.0343$ reaching a minimum at $t \cong 35(1/\omega_p)$ after which the mode amplitude shows oscillations. With the rather small collision frequencies of $v_0 = 0.001$ and 0.005 the mode is initially damped at rates $\gamma = -0.0382$ and $\gamma = -0.0401$ reaching minimum values at about $t \cong 35(1/\omega_p)$ after which the mode grows at rates $\gamma = 0.0172$ and $\gamma = 0.0162$ respectively. With larger collision frequencies $v_0 = 0.02$, 0.05, and 0.2 damping occurs throughout the simulation. The mode is initially damped at rates $\gamma = -0.0419$, $\gamma = -0.0483$, and $\gamma = -0.0883$ which later slacken off to $\gamma = -0.0269$, $\gamma = -0.0334$, and $\gamma = -0.0811$, respectively. In all the simulations the distribution function remains smooth and symmetric and the total energy is conserved to within 0.1%.

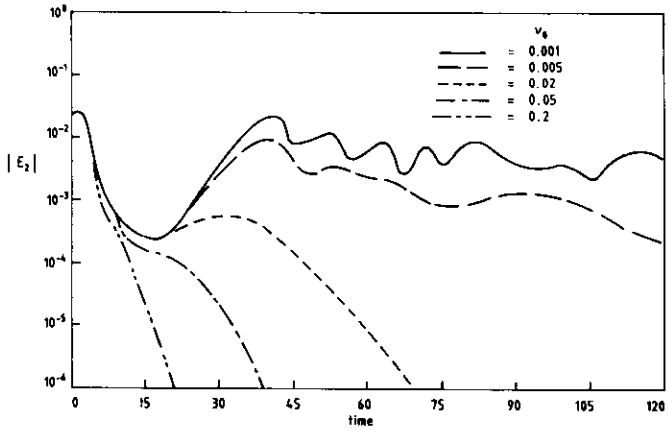

FIG. 5. Non-linear Landau damping. Electrostatic mode $|E_2|$, $k = 0.5$, $A = 0.5$, $N_x = 32$, $N_v = 128$, $L = 12.554$, $v_{max} = 5.0$, and $dt = 0.125$. Collision frequencies $v_0 = 0.001, 0.005, 0.02, 0.05, 0.2$.

We also studied non-linear Landau damping using a somewhat larger initial perturbation. In this case we use the parameters $A = 0.5$ and $k = 0.5$, so that the plasma length is $L = 12.5664$. There are 32 elements in the x direction and 128 in the v direction, $v_{max} = 7.0$. A velocity dependent collision frequency (32) is used and v_0 is given the values 0.0, 0.001, 0.005, 0.02, 0.05, and 0.2. The collisionless results agree well with those reported earlier [7] which had an initial decay of $\gamma = -0.281$ with a minimum reached at $t = 15.3(1/\omega p)$, followed by growth at $\gamma = 0.084$ until about $t = 40(1/\omega p)$. Graphs showing the variation in the envelop of the first electrostatic mode for the simulations are given in Fig. 4. For the smaller collision frequencies $v_0 = 0.001$ and 0.005 the curves show an initial decay at approximately equal rates of $\gamma = -0.289$, -0.291 with a minimum being reached at about $t = 15(1/\omega p)$; a period of growth follows with $\gamma = 0.0813$, 0.0796, respectively, up to a time of about $t = 40(1/\omega p)$ and then there is slow amplitude oscillation. With the larger frequencies of $v_0 = 0.02$, 0.05, and 0.2 the curves show an initial rapid decay at the rates $\gamma = -0.316$, $\gamma = -0.332$, and $\gamma = -0.353$, respectively, up to a time $t \cong 12$, after which there is no growth but damping continues at the reduced rates of $\gamma = -0.157$, $\gamma = -0.191$, and $\gamma = -0.213$.

For the second electrostatic mode similar observations are made; see Fig. 5. With $v_0 = 0.001$ and 0.005 there is a period of decay at rates $\gamma = -0.564$, -0.566 with a minimum being reached at about $t = 12(1/\omega p)$ followed by growth at $\gamma = 0.216$, 0.209 with a maximum being reached at about $t = 40(1/\omega p)$. Amplitude oscillations then occur with some superimposed damping when $v_0 = 0.005$. With the larger collision frequencies there is again an initial period of rapid decay at approximately the same rate of about $\gamma = -0.761$, followed by further decay at reduced rates. Only when $v_0 = 0.02$ is slight growth observed, sandwiched between these periods of decay.

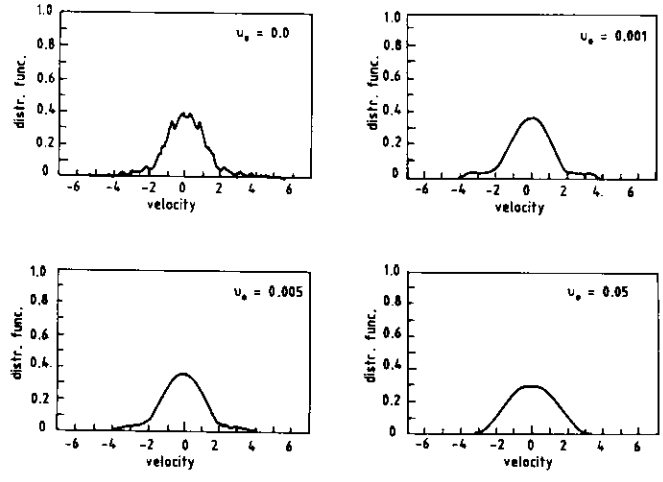

FIG. 6. Non-linear Landau damping. Distribution functions at $t = 120(1/\omega_p)$ for $v_0 = 0$, 0.001, 0.005, and 0.05.

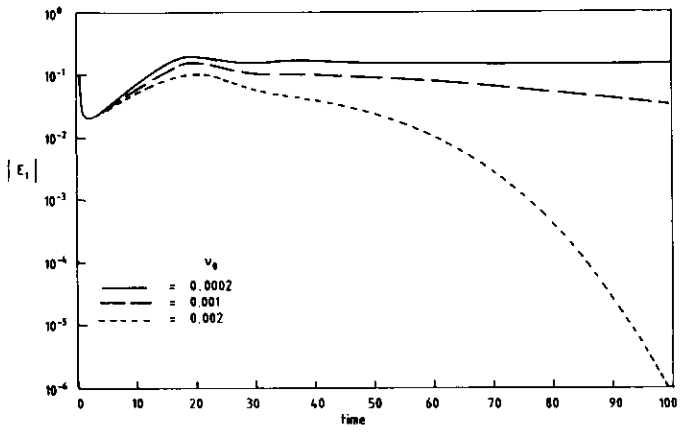

FIG. 7. Two stream instability. The effect of a non-zero collision frequency ν_0 on the amplitude envelope of $|E_1|$, $k = 0.5$, $A = 0.05$, $N_x = 32$, $N_v = 128$, $L = 12.5664$, $v_{\max} = 5.0$, and $dt = 0.125$. Collision parameters $\nu_0 = 0.0002, 0.001, 0.002$.

The third electrostatic mode follows a similar pattern. With $\nu_0 = 0$, 0.001, and 0.005 there is an initial period of decay at rates $\gamma = -1.031, -1.042, -1.042$ with a minimum being reached at about $t = 12(1/\omega p)$ followed first by growth and finally by amplitude oscillations with some superimposed damping when $\nu_0 = 0.005$. With the larger collision frequencies there is again an initial period of rapid decay at approximately the same rate of $\gamma = -1.042$, followed by further decay at reduced rates. Only when $\nu_0 = 0.02$ is slight growth observed sandwiched between these periods of decay.

A pronounced effect is observed on the distribution function as shown in Fig. 6. In the collisionless case, $\nu_0 = 0$, it remains Maxwellian but a wavy structure develops and grows on the main body of the distribution function and persists throughout the simulation [7, 8, 12]. For non-zero ν_0 the wavy structure is smoothed out and for the larger values of ν_0 the distribution function broadens in a fashion similar to that observed in simulations of collisional heating of plasmas by ac and dc electric fields [10]. For the smaller collision frequencies $\nu_0 = 0.001$ and 0.005 shoulders develop on the distribution function.

When the Maxwellian distribution function (30) is replaced by the equilibrium distribution function (31) we find $\langle v_0^2 \rangle \sim 1.006$ and $D \sim 0.57$. With $A = 0.05$, $k = 0.3535$, and $\nu_0 = 0.001$ the fundamental electrostatic mode initially damps at a very low rate $\gamma \cong -0.0143$ reaching a minimum at $t \cong 35(1/\omega p)$, after which the amplitude shows slow oscillations, while with $A = 0.5$, $k = 0.5$, and $\nu_0 = 0.005$ the same mode is initially damped with rate $\gamma \cong -0.258$ reaching a minimum at $t \cong 10(1/\omega p)$, after which the mode grows at a rate $\gamma \cong 0.063$ attaining a maximum at $t \cong 40(1/\omega p)$. The mode amplitude then oscillates while being slowly damped. The distribution function remains unchanged in shape and form throughout the entire simulation.

As a second example we study the symmetric "two stream instability." The initial $f_0(x, v, 0)$ is again given by (33) while $f_0(v)$ takes the form

$$f_0(v) = \frac{v^2}{\sqrt{2}\,\pi} \exp\left(-\frac{v^2}{2}\right). \tag{34}$$

In this case the measured values of $\langle v_0^2 \rangle$ and D are $\langle v_0^2 \rangle = 3.0$ and $D = 2.26$. The "two stream instability" has been widely studied, and to facilitate comparison with earlier work [6, 7, 12, 21] we have chosen the parameter values $k = 0.5$ and $A = 0.05$, plasma length $L = 12.5664$, and 32×128 finite elements are used. When velocity *independent* collision frequencies with values $\nu_0 = 0$, 0.001 are used, the simulations produce results in complete agreement with those reported earlier [6, 7].

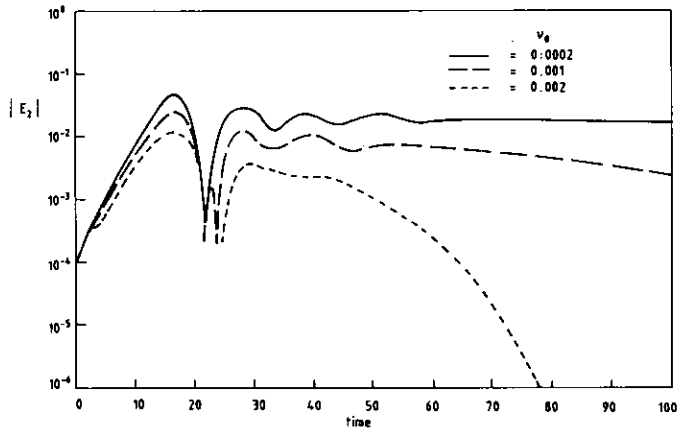

FIG. 8. Two stream instability. The effect of a non-zero collision frequency ν_0 on the amplitude envelope of $|E_2|$, $k = 0.5$, $A = 0.05$, $N_x = 32$, $N_v = 128$, $L = 12.5664$, $v_{\max} = 5.0$, and $dt = 0.125$. Collision parameter $\nu_0 = 0.0002, 0.001, 0.002$.

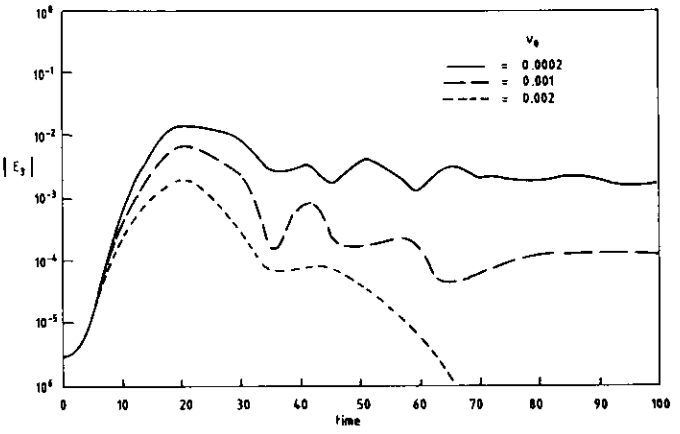

FIG. 9. Two stream instability. The effect of a non-zero collision frequency ν_0 on the amplitude envelope of $|E_3|$, $k = 0.5$, $A = 0.05$, $N_x = 32$, $N_v = 128$, $L = 12.5664$, $v_{\max} = 5.0$, and $dt = 0.125$. Collision parameters $\nu_0 = 0.0002, 0.001, 0.002$.

In Figs. 7–9 we present graphs showing how the envelope of the amplitude of the first three harmonics of the electric field are affected by velocity *dependent* collision frequencies of form (32) taking $v_0 = 0.0002$, 0.001, and 0.002. The initial transients are apparently little affected by collisions, whereas the following stages show damping in amounts dependent on the magnitude of v_0. When $v_0 = 0.0002$ almost no damping is observable in the graphs of the electric field modes but the field energy curves do show some damping. With $v_0 = 0.001$ there is moderate damping of the electric field mode amplitudes and of the field energy, which becomes severe for $v_0 = 0.002$. For collisionless cases [7, 12, 21] it has been observed that the valley between the two streams of electrons gradually fills in and that the distribution function develops some rather lumpy features. Our results confirm the first observation also for non-zero v_0 but we find, even with a very small non-zero collision frequency, that the distribution function remains smooth and symmetric and does not become lumpy. Rathmann and Denavit [10] observe, for the two stream instability in a spatially homogeneous plasma with no internal electric field, that the two beams eventually relax into a single broad beam. This tendency for the two beams to coalesce is also found in the present simulations, as shown in Fig. 10. The relaxation process is complete by $t = 80(1/\omega_p)$ for a collision frequency of 0.005 while for smaller values such as $v_0 = 0.0001$ the beams are still distinct by the end of the run at $t = 200(1/\omega_p)$.

The solution of Eqs. (8) and (9) involve advection which generally tends to generate spurious oscillations and negative values of the distribution function near large gradients. It is thought that the collision operator may well help to alleviate this problem. To examine this idea a two stream instability arising from two cold electron beams is studied. The initial condition approximates

$$f_0(v, 0) = \frac{1}{2\Delta v}\left[\delta(x - 1.25) + \delta(x + 1.25)\right].$$

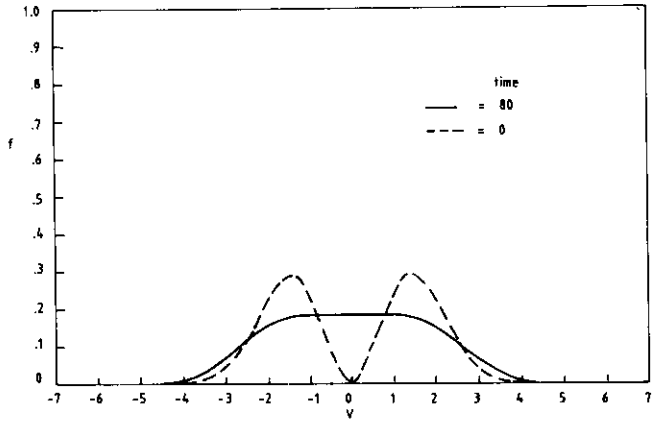

FIG. 10. Two stream instability. Distribution function compared at times $t = 0$, $80(1/\omega_p)$. Collision frequency $v_0 = 0.005$.

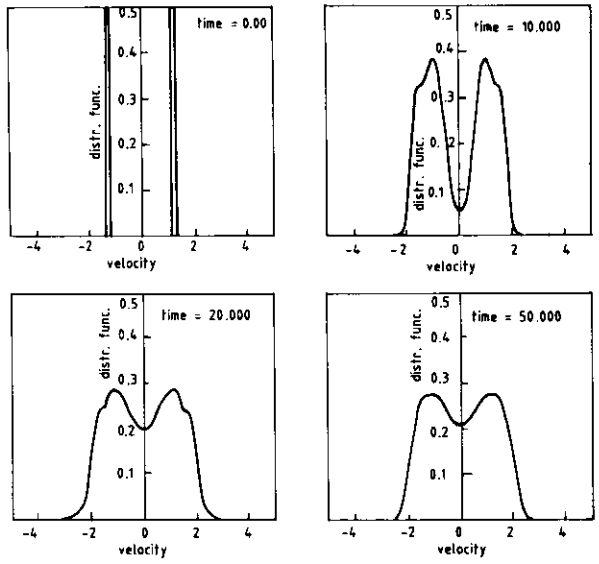

FIG. 11. Two stream instability: cold beams. Evolution of the distribution function. Collision parameter $v_0 = 0.002$.

The actual distribution function comprises two triangular areas each of height, $1/2\Delta v = 6.4$, based on two adjacent finite elements; see Fig. 11. This configuration leads to very steep gradients and poses a severe test for the algorithm. Parameters include $k = 0.5$, $A = 0.05$, plasma length $L = 12.5664$, $v_{max} = 5.0$, and 32×128 finite elements are used.

For the collisionless case, $v_0 = 0$, the distribution function fragments, spreads rapidly to the edges of the region, and the simulation comes to a premature end at $t = 32.5(1/\omega_p)$. A small collision frequency, $v_0 = 0.0002$, stabilises the simulation to some extent so that it proceeds to completion

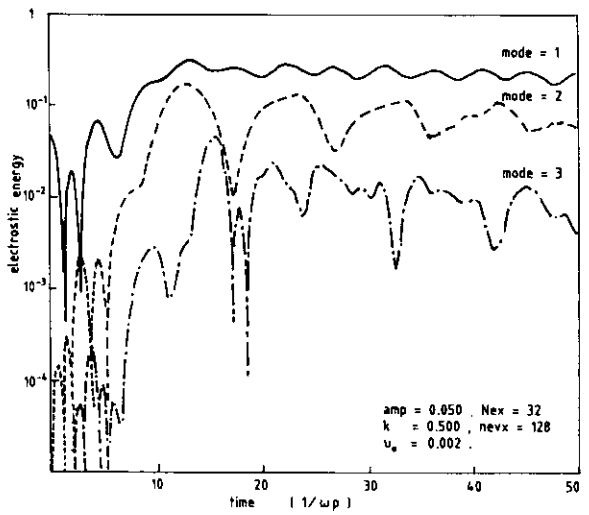

FIG. 12. Two stream instability: cold beams. The evolution of the amplitudes of modes 1 to 3 of the electrostatic energy. Plasma dimensions $L = 12.5664$, $v_{max} = 5.0$, $dt = 0.125$. Collision parameter $v_0 = 0.002$.

at $t = 50(1/\omega_p)$. Fragmentation has been halted but spurious oscillations still develop and the function spreads to the edges of the region. With a larger value, $v_0 = 0.002$, we obtain the results given in Figs. 11 and 12. The amplitudes of the electrostatic modes, Fig. 12, vary temporarily in a way similar to those observed in collisionless simulations with a Maxwellian $f_0(v)$; see Fig. 6 of Ref. [7]. Figure 11 shows that the collision operator has influenced the distribution function, causing it to spread out uniformly, leading at $t = 50(1/\omega_p)$ to a doubly humped distribution very similar in form to that found with a Maxwellian initial condition; cf. Fig. 8 of Ref. [7]. The larger collision frequency has suppressed the development of spurious oscillations on the distribution function arising from the rather extreme initial conditions. These oscillations can also be controlled by increasing the number of finite elements in the regions where large gradients are observed.

6. DISCUSSION

Here we have developed a splitting technique within a locally one-dimensional finite element method to solve the Fokker–Planck equation for an electron plasma with a homogeneous background plasma of ions. A one-dimensional collision operator of the type suggested by Lenard and Bernstein [2] in which the collision frequency may be a function of velocity, allowing Coulomb collisions to be modelled, has been incorporated into the computer code. The algorithm is unconditionally stable, conserves particle numbers, and an appropriate form for the diffusion coefficient ensures that it is energy conserving. This scheme has been used to simulate linear and non-linear Landau damping of plasma waves and the symmetric two stream instability. We have demonstrated that the method reproduces in detail the physics of the phenomena investigated, producing results confirming and extending earlier numerical observations.

In the simulations reported here the energy conservation for all simulations was better than 0.1%. An operation count for the one-dimensional algorithm shows it to require approximately $(34N_xN_v)$ $\times/\div$ and $(52N_xN_v)$ $+/-$ per timestep, where N_x, N_v are large. This count is similar to that for Rathman and Denavit's particle code based algorithm [10], which also requires a count proportional to N_xN_v and which is much less than needed by the two-dimensional algorithm [12].

The advantages of the present locally one-dimensional scheme in the solution of the simplified Fokker–Planck equation lie in its simplicity and efficiency. It can be extended to more complicated problems in higher dimensions of space or velocity and to more general boundary conditions. Using this approach, two- or three-dimensional simulations with the simplified Fokker–Planck equation are feasible by reduction of the original problem to a series of one-dimensional problems.

REFERENCES

1. S. Chandrasekhar, *Rev. Modern Phys.* **15**, 1 (1943).
2. A. Lenard and I. B. Bernstein, *Phys. Rev.* **112**, 1456 (1958).
3. E. C. Taylor and C. G. Comisar, *Phys. Rev.* **132**, 2379 (1963).
4. J. Denavit, *Phys. Fluids* **28**, 2773 (1985).
5. J. Denavit, B. W. Doyle, and R. H. Hirsch, *Phys. Fluids* **11**, 2241 (1969).
6. T. Armstrong and D. Montgomery, *J. Plasma Phys.* **1**, 425 (1968).
7. C. Z. Cheng and C. Knorr, *J. Comput. Phys.* **22**, 330 (1976).
8. V. E. Zakarov and V. I. Karpman, *Sov. Phys. JEPT* **16**, 351 (1963).
9. J. Killeen and K. D. Marx, in *Methods in Computer Phys.*, edited by B. Alder, S. Fernbach, and M. Rotenberg (Academic Press, New York, 1970), Vol. 9, p. 422.
10. C. E. Rathmann and J. Denavit, *J. Comput. Phys.* **18**, 165 (1975).
11. T. A. Mehlhorn and J. J. Duderstadt, *J. Comput. Phys.* **38**, 86 (1980).
12. S. A. Zaki, L. R. T. Gardner, and T. J. M. Boyd, *J. Comput. Phys.* **79**, 184 (1988).
13. V. V. U. Erz, Ph.D. thesis, Institut für Plasmaforschung der Universität Stuttgart, 1981 (unpublished).
14. L. R. T. Gardner and G. A. Gardner, in *Numer. Methods Non-Linear Problems*, edited by C. Taylor, D. R. J. Owen, E. Hinton, and D. B. Damjanac (Pineridge, Swansea, 1986), Vol. 3, p. 811.
15. D. J. Peaceman and H. H. Rachford, *Trans. Am. Math. Soc.* **82**, 421 (1956).
16. S. I. Marchuk, *Methods of Numerical Mathematics* (Springer-Verlag, Berlin, 1975).
17. L. Hayes, *Int. J. Numer. Methods Eng.* **16**, 35 (1980).
18. W. P. Gula and C. K. Chu, *Phys. Fluids* **16**, 1135 (1973).
19. J. Canosa, *J. Comput. Phys.* **13**, 158 (1973).
20. L. R. T. Gardner, G. A. Gardner, and S. I. Zaki, in *Proceedings, Int. Conf. Signals and Systems, Brighton, Vol. 4, 14, 1989.*
21. T. P. Armstrong and D. Montgomery, *Phys. Fluids* **12**, 2094 (1970).